

Quantized adiabatic quantum pumping due to interference

O. Entin-Wohlman and Amnon Aharony

*School of Physics and Astronomy, Raymond and Beverly Sackler Faculty of Exact Sciences,
Tel Aviv University, Tel Aviv 69978, Israel*

Vyacheslavs Kashcheyevs

Institute of Solid State Physics, University of Latvia, 8 Kengaraga St., LV-1063 Riga, Latvia.

(October 30, 2018)

Recent theoretical calculations, demonstrating that quantized charge transfer due to adiabatically modulated potentials in mesoscopic devices can result purely from the interference of the electron wave functions (without invoking electron-electron interactions) are reviewed: (1) A new formula is derived for the pumped charge Q (per period); It reproduces the Brouwer formula without a bias, and also yields the effect of the modulating potential on the Landauer formula in the presence of a bias. (2) For a turnstile geometry, with time-dependent gate voltages $V_L(t)$ and $V_R(t)$, the magnitude and sign of Q are determined by the relative position and orientation of the closed contour traversed by the system in the $\{V_L - V_R\}$ plane, relative to the transmission resonances in that plane. Integer values of Q (in units of e) are achieved when a transmission peak falls inside the contour, and are given by the winding number of the contour. (3) When the modulating potential is due to surface acoustic waves, Q exhibits a staircase structure, with integer values, reminiscent of experimental observations.

I. INTRODUCTION

When parameters of the Hamiltonian are slowly varied as function of time, adiabatic control of the electronic states becomes possible. When the change is carried out periodically, such that the Hamiltonian returns to itself after each cycle, one may pump an integral number, \mathcal{N} , of electrons through the system during each cycle. This results in a direct current (dc), flowing in response to an ac signal, which, when averaged over a cycle, is proportional to the modulation frequency times $\mathcal{N}e$ (e being the electronic charge).¹ Such adiabatic control of system parameters may be realized in nanostructures, where either the shape-forming potential, or the tunnel couplings between the structure and the leads (connected to the electronic reservoirs) can be modulated in a controllable way.

The possibility to transmit an integral number of electrons per cycle through an unbiased system, has been realized in two systems: 1. Quantum-dot devices, connected to leads via point contacts having small conductances which were modulated in time (turnstile devices);^{2,3} 2. Surface-acoustic-wave-based devices.⁴ In both examples, the observed quantization has been attributed to the Coulomb blockade, which quantizes the number of electrons on the device. However, the possibility to achieve quantization in ‘open’ nanostructures is much more intriguing. In such geometries, the electrons are not confined to a certain region but are rather spread over the entire device. Then, Coulomb-blockade effects are expected to play a minor role; The question hence arises whether quantum interference of the electronic wave function suffices to produce quantization (as originally proposed by Thouless¹).

Here we explore the conditions for the charge pumped during a period, Q , to be (almost) quantized, due to interference effects alone, without invoking electron-electron interactions. Our discussion begins (in Sec. 2) with the derivation of the expression for Q , which serves to put limitations on the validity of the widely-used adiabatic approximation. We continue (in Sec. 3) with an analysis of the turnstile geometry. That discussion points out to the connection between the conditions for resonance transmission and integral values of Q . In Sec. 4 we discuss the pump based on the surface acoustic waves (SAW’s). Finally, Sec. 5 includes concluding remarks.

II. TRANSPORT THROUGH A PERIODICALLY-MODULATED SYSTEM

Consider a ballistic nanostructure of arbitrary geometry, connected by leads (denoted by α) to electronic reservoirs having the chemical potentials μ_α , and subject to a potential modulated periodically in time. The current flowing through this system will be obtained by first finding the time-dependent scattering states, and then using them to obtain the current.

The required time-dependent scattering solutions are derived from a systematic expansion in the temporal derivatives of the instantaneous solutions (that is, the scattering solutions of the Hamiltonian in which time is ‘frozen’). The first-order of this expansion yields the ‘adiabatic approximation’.⁵ This expansion procedure necessitates that the characteristic inverse time-constant, $1/\tau$, which describes the time dependence of the modulating potential, will be smaller than any characteristic energy scale of the electrons. However, it turns out that the

expansion also requires that the amplitude of the modulating potential will be small.

Let the system be described by the Hamiltonian

$$\mathcal{H}(\mathbf{r}, t) = \mathcal{H}_0(\mathbf{r}) + V(\mathbf{r}, t), \quad (1)$$

where the potential $V(\mathbf{r}, t)$ is assumed to be confined in space, so that asymptotic behaviors of the scattering solutions can be clearly defined. The Hamiltonian \mathcal{H}_0 consists of the kinetic energy. As in the usual scattering treatment, we seek for the scattering state $\Psi_{\alpha n}$, which is excited by the free wave $w_{\alpha n}^-$ (incoming in the transverse mode n of lead α with energy E), which is normalized to carry a unit flux,

$$\Psi_{\alpha n}(\mathbf{r}, t) = e^{-iEt} \left(w_{\alpha n}^-(\mathbf{r}) + \tilde{\chi}_{\alpha n}(\mathbf{r}, t) \right). \quad (2)$$

By inserting this form into the time-dependent Schrödinger equation, (noting that $w_{\alpha n}^-$ is a solution of \mathcal{H}_0), $\tilde{\chi}_{\alpha n}$ can be written in terms of the instantaneous Green function, $G^t(E)$,

$$\left(E - \mathcal{H}(\mathbf{r}, t) \right) G^t(E; \mathbf{r}, \mathbf{r}') = \delta(\mathbf{r}' - \mathbf{r}), \quad (3)$$

as follows

$$\left(G^t \right)^{-1} \tilde{\chi}_{\alpha n}(\mathbf{r}, t) = V(\mathbf{r}, t) w_{\alpha n}^-(\mathbf{r}) - i \frac{\partial \tilde{\chi}_{\alpha n}(\mathbf{r}, t)}{\partial t}. \quad (4)$$

Note that the time dependence of the scattered wave function, $\tilde{\chi}_{\alpha n}(\mathbf{r}, t)$, has the same characteristic time scale as V : e.g., when the modulating potential is oscillating in time with frequency ω , $\tilde{\chi}$ contains all harmonics.

Equation (4) is solved iteratively: the temporal derivative appearing on the right-hand-side is regarded as a small correction. The zero-order, $\chi_{\alpha n}^t$, is the scattering solution of the instantaneous Hamiltonian (in which time appears as a parameter),

$$\chi_{\alpha n}^t(\mathbf{r}) = w_{\alpha n}^-(\mathbf{r}) + \int d\mathbf{r}' G^t(E; \mathbf{r}, \mathbf{r}') V(\mathbf{r}', t) w_{\alpha n}^-(\mathbf{r}'). \quad (5)$$

Then the scattering solution read

$$\chi(\mathbf{r}, t) = \chi^t(\mathbf{r}) + \chi^{(1)}(\mathbf{r}, t) + \chi^{(2)}(\mathbf{r}, t) + \dots, \quad (6)$$

with the first-order

$$\chi^{(1)}(\mathbf{r}, t) = -i \int d\mathbf{r}' G^t(E; \mathbf{r}, \mathbf{r}') \dot{\chi}^t(\mathbf{r}'), \quad (7)$$

and the second-order

$$\chi^{(2)}(\mathbf{r}, t) = -i \int d\mathbf{r}' G^t(E; \mathbf{r}, \mathbf{r}') \Delta \dot{\chi}^t(\mathbf{r}'), \quad (8)$$

where

$$\Delta \dot{\chi}^t(\mathbf{r}') = -i \int d\mathbf{r}'' \frac{d}{dt} \left(G^t(E; \mathbf{r}', \mathbf{r}'') \dot{\chi}^t(\mathbf{r}'') \right). \quad (9)$$

and $\dot{\chi}_{\alpha n}^t \equiv d\chi_{\alpha n}^t/dt$. Hence, in our iterative solution, the time-dependent scattering states are given entirely in terms of the *instantaneous* solutions of the problem at hand.

In the scattering formalism⁶⁻⁸ the thermal average of the current density operator is given by

$$\langle \mathbf{j}(\mathbf{r}, t) \rangle = \frac{e}{m} \Im \int \frac{dE}{2\pi} \sum_{\alpha n} f_{\alpha}(E) \chi_{\alpha n}^*(\mathbf{r}, t) \frac{\partial \chi_{\alpha n}(\mathbf{r}, t)}{\partial \mathbf{r}}, \quad (10)$$

where $f_{\alpha}(E)$ is the Fermi distribution in the reservoir connected to the α lead. Evaluating $\langle \mathbf{j}(\mathbf{r}, t) \rangle$ as \mathbf{r} approaches ∞ in lead β , and then integrating over the cross-section of that lead yields the current $I_{\beta}(t)$ flowing into lead β^9 . In the following, we analyze this current, confining for simplicity the discussion to a nanostructure connected to left (ℓ) and right (r) leads.

A. The adiabatic approximation

Consider first the net current passing through the system utilizing the adiabatic approximation, that is, keeping only the term (7). Then the current flowing during a single period of the modulating potential is⁹

$$I = \oint \frac{dt}{\tau} \left(I_{\ell}(t) - I_r(t) \right) = I_{\text{bias}} + I_{\text{pump}}. \quad (11)$$

The first part, I_{bias} , flows only when the system is biased,

$$\begin{aligned} I_{\text{bias}} = e \oint \frac{dt}{\tau} \int \frac{dE}{2\pi} & \left(f_{\ell}(E) - f_r(E) \right) \\ & \times \sum_{nm} \left[2 |S_{rm, \ell n}^t|^2 + \Re \left(S_{\ell m, \ell n}^t U_{\ell m, \ell n}^* - S_{\ell m, rn}^t U_{\ell m, rn}^* \right. \right. \\ & \left. \left. - S_{rm, \ell n}^t U_{rm, \ell n}^* + S_{rm, rn}^t U_{rm, rn}^* \right) \right], \quad (12) \end{aligned}$$

where $U_{\beta m, \alpha n} = \int d\mathbf{r} \chi_{\beta m}^t(\mathbf{r}) \dot{\chi}_{\alpha n}^t(\mathbf{r})$, and $S_{\beta m, \alpha n}^t$ is the matrix element of the instantaneous scattering matrix. Equation (12) can be considered as a generalization of the Landauer formula, extended to include the effect of a time-dependent potential in the adiabatic approximation. The second part of the current, I_{pump} , is established by the time-dependent potential (though it is affected by the chemical potential difference, when the latter is applied). Explicitly,

$$\begin{aligned} I_{\text{pump}} = e \oint \frac{dt}{\tau} \int \frac{dE}{2\pi} & \frac{\partial (f_{\ell}(E) + f_r(E))}{\partial E} \\ & \times \frac{1}{2} \sum_m \left[\langle \chi_{\ell m}^t | \dot{V} | \chi_{\ell m}^t \rangle - \langle \chi_{rm}^t | \dot{V} | \chi_{rm}^t \rangle \right]. \quad (13) \end{aligned}$$

It can be shown⁹ that the terms in the square brackets of (13) reproduce the Brouwer¹⁰ formula, derived for an unbiased system (in which I_{pump} is given in terms of temporal derivatives of the instantaneous scattering matrix).

B. Corrections to the adiabatic approximation

When the second-order in the expansion (6) is retained, one obtains the first correction to the widely-used adiabatic approximation. We will discuss here the pumping current beyond the adiabatic approximation for an unbiased system connected to two single-channel leads. In that case, the current entering lead β , \tilde{I}_β , is⁹

$$\tilde{I}_\beta(t) = \frac{e}{2\pi} \int dE \left(\frac{\partial f(E)}{\partial E} \right) \left[\langle \chi_\beta^t | \dot{V} | \chi_\beta^t \rangle + \Im \left(\langle \chi_\beta^t | 2\dot{V}(t) \hat{G}^t(E) + \ddot{V}(t) G^t(E) | \chi_\beta^t \rangle \right) \right]. \quad (14)$$

The first term in the square brackets is the adiabatic approximation result. The second arises from the second-order correction (8) to the scattering state.

The relative magnitude of the correction compared to the leading-order term may be accessed by noting that⁹

$$\langle \chi_\beta^t | 2\dot{V}(t) \hat{G}^t(E) + \ddot{V}(t) G^t(E) | \chi_\beta^t \rangle = - \langle \chi_\beta^t | 2\dot{V} G^t(E) \dot{V} + \ddot{V} | \frac{\partial \chi_\beta^t}{\partial E} \rangle. \quad (15)$$

Hence, the validity of the adiabatic approximation is not only restricted by the smallness of $1/\tau$ dominating the temporal derivatives. It depends as well on the energy derivatives of the scattering states (i.e., the energy scale of the instantaneous reflection and transmission amplitudes) and the strength of the modulating potential itself: For the adiabatic approximation to be valid, one should have $V\tau \ll 1$.¹¹ Below, we evaluate the pumping current in the adiabatic approximation, keeping the above restrictions in mind.

III. INTERFERENCE EFFECTS AND QUANTIZED PUMPING IN A MODULATED TURNSTILE DEVICE

Here we investigate the turnstile pump, and in particular focus on the correlation between resonant transmission and the magnitude of adiabatically pumped charge. This correlation has been pointed out by Levinson *et al.*¹² and by Wei *et al.*¹³ The idea may be summarized generically as follows.¹⁴ Consider a quantum dot, connected to its external leads by two point contacts, whose conductances are controlled by split-gate voltages which are modulated periodically in time. During each cycle the system follows a closed curve, the ‘pumping contour’, in the parameter plane spanned by the point contact conductances. As the system parameters are varied (for example, the gate voltage on the dot) the pumping contour distorts and shifts, forming a Lissajous curve in the parameter plane. The pumped charge will be (almost) quantized when the pumping contour encircles transmission peak(s) (that is, resonances) of the quantum dot in that parameter plane. Its magnitude (in units of the electronic charge, e) and sign are determined by the winding number of the pumping contour.

This connection between resonant transmission and pumping may be explored by studying a simple model. Employing the tight-binding description, we imagine the quantum dot to be coupled to semi-infinite 1D (single-channel) leads by matrix elements J_ℓ and J_r . Those are oscillating in time with frequency ω , such that the modulation amplitude is P and the phase shift between the J_ℓ modulation and that of J_r is 2ϕ ,

$$\begin{aligned} J_\ell &= J_L + P \cos(\omega t + \phi), \\ J_r &= J_L + P \cos(\omega t - \phi). \end{aligned} \quad (16)$$

The point contact conductances are then given (in dimensionless units) by $X_\ell \equiv J_\ell^2$ and $X_r \equiv J_r^2$. As the couplings of the quantum dot to the leads are modulated in time, J_ℓ and J_r can attain both negative and positive values. This reflects a modulation of the potential shaping the dot: The tight-binding parameters J_ℓ and J_r , which are derived as integrals over the site ‘atomic’ wave functions and the oscillating potential, can have both signs. The extreme modulation arises for $J_L = 0$, when the hopping matrix elements which couple the dot to the leads oscillate in the range $\{-P, P\}$. The conductances of the point contacts are then modulated in the range $\{0, P^2\}$. The corresponding Lissajous curve of the pumping is then a simple closed curve. Another possibility is to keep the couplings finite at any time, i.e., $J_L \neq 0$, and to modulate the couplings around this value. In that case the Lissajous curve may fold on itself [compare Figs. 2 and 3 below]. This yields a rather rich behavior of the pumped charge.

The quantum dot is modeled by a ‘bunch’ of tight-binding sites connected among themselves. For simplicity, we take the latter in the form of a finite chain of N sites, each having the on-site energy ϵ_0 , and attached to its nearest-neighbor with a transfer amplitude $-J_D$. This structure is connected to electronic reservoirs by two 1D chains of sites, whose on-site energies vanish, and whose nearest-neighbor transfer amplitudes are denoted by $-J$. The Fermi energy of an electron of wave vector k moving on the leads is

$$E_k = -2J \cos ka, \quad (17)$$

where a is the lattice constant.

In the adiabatic approximation, the charge, Q , pumped through the quantum dot during a single period of the modulation is given by (13) as follows

$$Q = \frac{e}{4\pi} \oint dt \left[\langle \chi_r^t | \dot{V} | \chi_r^t \rangle - \langle \chi_\ell^t | \dot{V} | \chi_\ell^t \rangle \right]. \quad (18)$$

(The limit of zero temperature is taken for simplicity; Obviously finite temperature will ‘smear’ the effect.¹²) The temporal derivative of the modulating potential in the present case is

$$\begin{aligned} \dot{V}(n, n') = & -\dot{J}_\ell \left(\delta_{n,1} \delta_{n',0} + \delta_{n',1} \delta_{n,0} \right) \\ & -\dot{J}_r \left(\delta_{n,N} \delta_{n',N+1} + \delta_{n',N} \delta_{n,N+1} \right). \end{aligned} \quad (19)$$

The expression (18) requires the knowledge of the instantaneous scattering states. These are easily derived. One writes those states in terms of the instantaneous reflection (r_t and r'_t) and transmission (t_t) amplitudes: For the scattering state incited by a free wave incoming from the left one has $\chi_\ell^t(x) = A_{0,\ell} [e^{ikx} + r_t e^{-ikx}]$ on the left lead, and $\chi_\ell^t(x) = A_{0,\ell} t_t e^{ikx}$ on the right lead, with $x = na$. Similarly, $\chi_r^t(x) = A_{0,r} [e^{-ikx} + r'_t e^{ikx}]$ on the right lead, and $\chi_r^t(x) = A_{0,r} t_t e^{-ikx}$ on the left lead, for the scattering state incited by a plane wave incoming from the right reservoir. For both, the normalization to a unit flux implies that $A_{0,\ell} = A_{0,r} = (2J \sin ka)^{-1/2}$. The reflection and transmission amplitudes are given by (all energies are scaled in units of J)

$$\begin{aligned} r_t e^{-i2ka} + 1 &= \left(e^{ika} X_\ell X_r \sin N_- qa - J_D X_\ell \sin N qa \right) M_k, \\ r'_t e^{i2Nka} + 1 &= \left(e^{ika} X_\ell X_r \sin N_- qa - J_D X_r \sin N qa \right) M_k, \\ t_t &= -e^{-ikN-a} J_\ell J_r J_D \sin qa M_k, \end{aligned} \quad (20)$$

with $N_\pm \equiv N \pm 1$, and

$$\begin{aligned} M_k = 2i \sin ka \left[J_D^2 \sin N_+ qa - J_D e^{ika} (X_\ell + X_r) \sin N qa \right. \\ \left. + e^{i2ka} X_\ell X_r \sin N_- qa \right]^{-1}. \end{aligned} \quad (21)$$

The wave vector q describes the propagation of the wave on the quantum dot, such that $E_k - \epsilon_0 = -2J_D \cos qa$. By using these expressions in (18) one finds that, as function of the modulating amplitude, (or alternatively the gate voltage on the dot), the pumped charge can vary as depicted, for example, in Fig. 1.

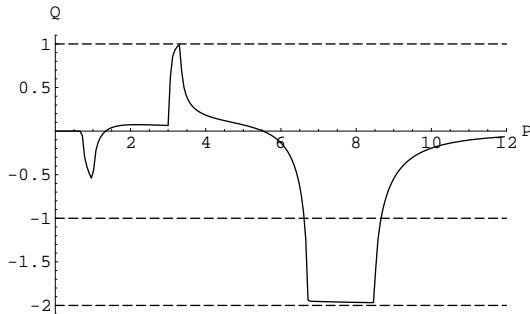


FIG. 1. The pumped charge, Q , in units of e , as function of the modulating amplitude, P . The parameters used are: $\epsilon_0 = 0$, $J_D = 1$, $J_L = 2$, $ka = 0.001\pi$, $N = 4$, and $\phi = 0.05$.

We next make the correspondence between the ‘quantized’ values of Q , as portrayed in Fig. 1, and the location of the pumping contour relative to the resonant transmission of the quantum dot. The transmission coefficient of our system, $T = |t_t|^2$, is [see Eq. (20)]

$$T = \left[1 + \frac{Z^2 + (J_D \sin ka \sin N qa (X_\ell - X_r))^2}{(2J_D \sin ka \sin qa)^2 X_\ell X_r} \right]^{-1}, \quad (22)$$

with $Z = J_D^2 \sin N_+ qa + \frac{E_k}{2} J_D \sin N qa (X_\ell + X_r) + X_\ell X_r \sin N_- qa$. Clearly, one has $T=1$ when $X_\ell = X_r$ and $Z=0$. For $N > 1$, these equations give two points on the diagonal in the $\{X_\ell - X_r\}$ plane. The maxima of T , when either X_ℓ or X_r is varied while the other parameter is kept fixed, occur on two ‘resonance lines’, shown in thick lines in Figs. 2 and 3. The figures also show the topology of the curve traversed by the system during the pumping cycle for representative values of P . In Fig. 2 we have $P=1$. The pumping contour encloses a small part of the upper resonance line, and also touches the peak on the lower resonance line. Indeed, Q has an intermediate value near -0.5 , decreasing to zero as P moves away from 1 (see Fig. 1).

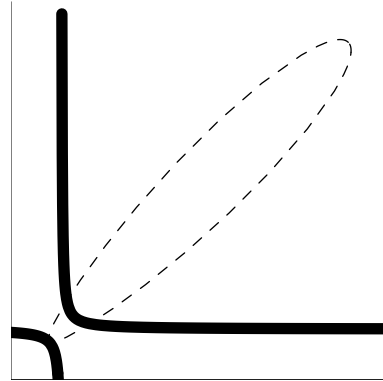


FIG. 2. The pumping contour (dashed line) and the resonance lines (thick lines), in the $\{X_\ell - X_r\}$ plane, for $P=1$.

Increasing the amplitude to the value $P=5$ reveals that the pumping contour encloses both peaks on the resonance lines, and therefore their separate contributions almost cancel one another, leading to a tiny value of Q . Also, the pumping curve begins to fold on itself, giving rise to the ‘bubble’ close to the origin (see Fig. 3). Following the increase of that bubble as P is enhanced leads to the situation in which the bubble encloses the lower resonance, and then the charge attains a unit value (see Fig. 1). As the bubble increases further, capturing the two resonance lines, Q again becomes very small. But upon further increasing P , we reach the interesting situation, depicted in Fig. 3 for $P=8$, in which the bubble encircles *twice* the upper resonance line, leading to a pumped charge very close to $|2e|$ (see Fig. 1).

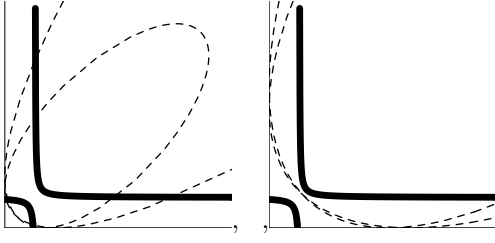


FIG. 3. Same as Fig. 2, for $P=5$ (left), $P=8$ (right).

Thus, the condition for obtaining integral values of the pumped charge is that the contour traversed by the system in the parameter plane spanned by the pumping parameters should encircle a significant portion of a resonance line in that plane. The magnitude and the sign of the pumped charge are determined by that portion, and by the direction along which the resonance line is encompassed. We emphasize that the pumping contour, as well as the resonance lines, can be determined experimentally.¹²

The reason for this topological description of adiabatic charge pumping can be traced back to the expression for the pumped charge, Eq. (18). The main contribution to the temporal integration there comes from the poles of the integrand. The same poles are also responsible for the resonant states of the nanostructure, that is, for the maxima in the transmission coefficient.^{12,14} One can imagine more complex scenarios: Including higher harmonics of ω in the time dependence of the point contact conductances can create more complex Lissajous contours, which might encircle portions of the resonance lines more times, yielding higher quantized values of the pumped charge.

IV. INTERFERENCE EFFECTS AND QUANTIZED PUMPING IN A QUANTUM CHANNEL MODULATED BY SURFACE ACOUSTIC WAVES

Modulation of the potential acting on a nanostructure may be also achieved through the piezoelectric effect of surface acoustic waves (SAW's), which is relatively large in GaAs. In the two-dimensional electron gas formed in GaAs-AlGaAs samples the potential created by the SAW is screened out. However, the SAW's are effective within a quasi-one-dimensional channel (where screening is diminished) defined in GaAs-AlGaAs samples. In the experiments,⁴ the time-average current exhibits steps between plateaus, at quantized values of integer $\times e(\omega/2\pi)$, (ω is the SAW frequency), as function of either the gate voltage on the quantum channel, or the SAW amplitude. Here we propose an explanation for this observation, in terms of interference of non-interacting electrons.^{15,16}

Unlike the turnstile-like case, the piezoelectric potential, $\mathcal{H}_{\text{SAW}}(\mathbf{r}, t) = P \cos(\omega t - \mathbf{q} \cdot \mathbf{r})$, generated by the SAW

oscillates with time everywhere inside the nanostructure. The induced average current (in the absence of bias), flows in the direction of the SAW wave vector, \mathbf{q} . A realistic treatment of the experimental geometry¹⁶ only allowed a calculation at low SAW amplitude, P , yielding $Q \propto P^2$. The screening of the piezoelectric potential in the wide banks of the channel is also difficult to treat exactly. In view of this it is useful to gain insight into the phenomenon by applying a simple model.¹⁵ A 1D channel, connected to 1D leads. The Fermi energy of an electron moving on the leads is then again given by (17), while the 'channel' Hamiltonian is

$$\mathcal{H}_{\text{osc}} = \sum_n \{ \epsilon_n(t) |n\rangle \langle n| - J_n (|n\rangle \langle n+1| + hc) \}, \quad (23)$$

with $J_n = J_D$ inside the channel, $1 \leq n \leq N-1$, and $J_0 = J_\ell$, $J_N = J_r$ for the 'contacts' with the leads. The electric field generated by the SAW's

$$\epsilon_n(t) = V + P \cos[\omega t - qa(n - n_0)] \quad (24)$$

acts only inside the channel. (Effects due to gradual screening, or reflections from the channel ends, can be incorporated as well.¹⁵) Here V represents the gate voltage and $P > 0$, so that ϵ_n has a maximum (minimum) in the center of the channel $n_0 = (N+1)/2$ at $t = 0$ ($\tau/2$).

The adiabatic approximation seems to be particularly adequate for SAW frequencies, as $\hbar\omega$ is small compared to the relevant electronic energy scales. We hence use (18), with \dot{V} there replaced by \mathcal{H}_{osc} . The required instantaneous scattering states are straightforwardly found; The resulting expression can be put in the form¹⁵

$$Q = \frac{eJ_\ell^2 \sin ka}{\pi J} \int_{-\tau/2}^{\tau/2} dt \sum_{n=1}^N \dot{\epsilon}_n |g_{n,1}|^2, \quad (25)$$

where the (time-dependent) matrix g is given by

$$(g^{-1}(E))_{n,n'} = E\delta_{n,n'} - (\mathcal{H}_{\text{osc}})_{n,n'} + \delta_{n,n'} e^{ika} (\delta_{n,1} J_\ell^2 + \delta_{n,N} J_r^2) / J. \quad (26)$$

Using the same notations, the instantaneous transmission coefficient of the quantum channel reads $T^t = 4|g_{N,1}|^2 (J_\ell J_r / J)^2 \sin^2 ka$. This has maxima, as function of $\cos \omega t$, at the N poles of $g_{N,1}$, i.e. at the zeroes of $D(\cos \omega t) \equiv \det g^{-1}$. The time-averaged transmission, $\bar{T} = \int_{-\tau/2}^{\tau/2} dt T^t / \tau$ thus exhibits peaks wherever such poles occur within the period $\tau = 2\pi/\omega$. Similarly, Q will have singularities whenever $\cos \omega t$ comes close to a zero of D within the integration. For small $(J_\ell^2 + J_r^2)/J$, these poles have small imaginary parts, and Q exhibits large changes as $\cos \omega t$ passes near such a pole. These steps occur exactly where \bar{T} has spikes, originating from the same poles. Thus, again, we find an intimate relation between 'quantized' values of the pumped charge, and resonant transmission.

Figure 4 shows Q/e vs. V , for $N = 10$ at zero temperature. The other parameters used are: $J_L \equiv J_\ell =$

$J_r = 0.4$, $P/J_D = 8$, $ka = \pi/100$, and the SAW wave length is taken to be 4 times the channel length. Several plateaus are clearly observed, with Q/e very close to an integer, $\mathcal{N} = 1, \dots, 5$. (We have found that, quite generally, the number \mathcal{N} of sharp plateaus is up to $\mathcal{N} = N/2$, with possibly several additional rounded peaks or spikes.) The steps, at $V_{\mathcal{N}}$, between these plateaus appear to be equidistant.¹⁵ For large N

$$V_{\mathcal{N}} \approx E_F \pm (P + 2J_D - \Delta(\mathcal{N} + \frac{1}{2})), \quad (27)$$

with $\Delta = qa\sqrt{2PJ_D}$, that is, as the SAW amplitude P increases, the steps move outwards and broaden, in apparently accordance with experiments.⁴

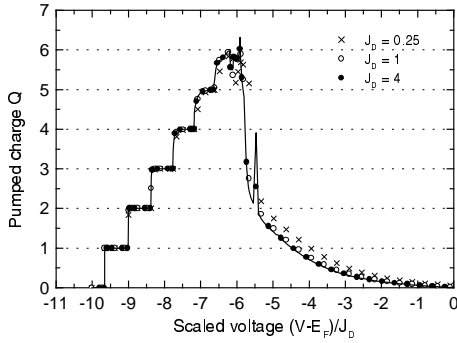


FIG. 4. The pumped charge *vs.* V . Energies are measured from the Fermi energy and scaled by J_D . This renders Q to depend on J_L^2/J_D alone.

Obviously, a finite pumped charge requires finite SAW amplitude P . Indeed, the steps become rounded as P , $|E_F - V|$ or qa decreases with the rounding beginning at the larger \mathcal{N} 's; The plateaus at $\mathcal{N} = \pm 1$ disappear last. These results remain robust¹⁵ over a wide range of ka , J_L and J_D , provided $0 < J_L^2/J \leq J_D \ll P$, $|E_F - V|$; As an example, Fig. 5 shows the effects of increasing J_D and J_L . As Eq. (27) implies, the staircase structure of Q is also obtained as function of P , at fixed V : Q remains very small up to $P_0 = E_F - V - 2J_D + \Delta/2$, exhibits $N/2$ steps, at intervals Δ (which now increases with P), and then decreases gradually towards zero. Thus, both V and P can be used for on-off switching of the pumped current.

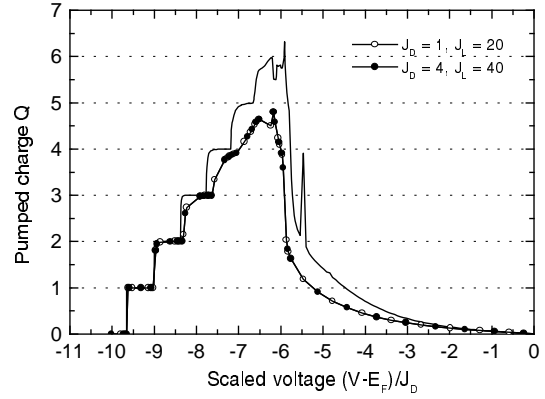


FIG. 5. The dependence of the pumped charge on the gate voltage, see text.

As mentioned above, the steps in Q are correlated with the spikes of the averaged transmission. It is interesting to follow these poles as function of the various parameters. Figure 6 depicts the partial charge $Q(t)$, resulting from integration of (25) only up to $t < \tau/2$, at different values of the gate voltage. As V increases through the first step at V_1 , $Q(t)$ suddenly exhibits a step from zero to one, which appears at $t = 0$. Upon further increasing V , this step moves to the left, and at $V = V_{\mathcal{N}}$, a new step (from $\mathcal{N} - 1$ to \mathcal{N}) enters at $t = 0$ (see the left panel of Fig. 6). Afterwards, there begin to enter steps of -1 , until at $V = E_F$ there are exactly $N/2$ steps of $+1$ followed by $N/2$ steps of -1 , yielding $Q = 0$ (the center panel of Fig. 6). A similar build-up of (negative) steps occurs starting from positive V -values which are then decreased, (right panel of Fig. 6). Thus, unlike the Coulomb blockade picture, in which \mathcal{N} electrons move together, carried by a single minimum of the moving potential, in the interference description, $Q(t)$ changes by discrete steps of 1, implying separate motion of the electrons, building up to \mathcal{N} after a full period. The step-like time dependence of $Q(t)$ implies the appearance of higher harmonics in ω , with amplitudes exhibiting staircase structure as well.¹⁵ Apparently, this will not be true in Coulomb-blockade-type description. Measurements of the induced current noise for the $\mathcal{N} > 1$ plateaus may be useful to distinguish between the simultaneous motion of \mathcal{N} electrons, and the single electron steps.⁴

To conclude this section, we note that even within this simple 1D model, it is possible to study effects arising from variations of the SAW amplitude P in space (due to screening effects, or to multiple reflections from the channel's ends), or from random energies $\{V_n\}$, which may represent impurities within the channel.

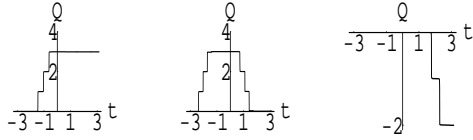


FIG. 6. Partial pumped charge Q in units of e , up to time t within a period, for different values of the gate voltage. The t -axis shows ωt between $-\pi$ and π . Here $P=8$, $N=6$, $J_D=1$, $J_L=0.4$, $qa=\pi/10$, and $ka=\pi/100$, and $V=-8.6, -2$, and 5.3 .

V. CONCLUDING REMARKS

Using simplified models, we have demonstrated that interference effects suffice to produce transfer of integral number of electrons through a mesoscopic (unbiased) system, subject to a periodically-varying potential. The calculations presented above utilize the expression for the pumped charge, Q , in the adiabatic approximation, that is, keeping only the first-order of the expansion (6). However, the next-order corrections need not be small; It is therefore an open question whether the quantization, and its relation to resonant transmission, will still be present when higher terms in the temporal expansion are retained.

ACKNOWLEDGEMENTS

We thank Y. Imry, Y. Levinson, and P. Wölfle for helpful conversations. This research was carried out in a cen-

ter of excellence supported by the Israel Science Foundation, and was supported in part by the Albert Einstein Minerva Center for Theoretical Physics at the Weizmann Institute of Science.

-
- ¹ D. J. Thouless: Phys. Rev. B **27** (1983) 6083; B. L. Altshuler and L. I. Glazman: Science **283** (1999) 1864.
 - ² L. P. Kouwenhoven *et al.*: Z. Phys. **B85** (1991) 381.
 - ³ M. Switkes *et al.*: Science **283** (1999) 381.
 - ⁴ J. M. Shilton *et al.*: J. Phys.: Condens. Matter **8** (1996) L531; V. I. Talyanskii *et al.*: Phys. Rev. B **56** (1997) 15180; A. M. Robinson *et al.*: Phys. Rev. B **65** (2002) 045313.
 - ⁵ J. E. Avron *et al.*: Phys. Rev. Lett. **87** (2001) 236601.
 - ⁶ Y. Levinson and P. Wölfle: Phys. Rev. Lett. **83** (1999) 1399.
 - ⁷ Y. Levinson: Phys. Rev. B **61** (2000) 4748.
 - ⁸ O. Entin-Wohlman, Y. Levinson, and P. Wölfle: Phys. Rev. B **64** (2001) 195308.
 - ⁹ O. Entin-Wohlman, A. Aharony, and Y. Levinson: Phys. Rev. B **65** (2002) 195411.
 - ¹⁰ P. W. Brouwer: Phys. Rev. B **58** (1998) R10135.
 - ¹¹ M. Wagner: Phys. Rev. A **51** (1995) 798.
 - ¹² Y. Levinson, O. Entin-Wohlman, and P. Wölfle: Physica A **302** (2001) 335.
 - ¹³ Y. Wei, J. Wang, and H. Gou: Phys. Rev. B **62** (2000) 9947; Y. Wei, J. Wang, H. Gou, and C. Roland: Phys. Rev. B **64** (2001) 115321.
 - ¹⁴ O. Entin-Wohlman and A. Aharony: Phys. Rev. B **66** (2002) 035329.
 - ¹⁵ A. Aharony and O. Entin-Wohlman: Phys. Rev. B **65** (2002) 241401; V. Kashcheyevs, A. Aharony, and O. Entin-Wohlman: unpublished.
 - ¹⁶ Y. Levinson, O. Entin-Wohlman, and P. Wölfle: Phys. Rev. Lett. **85** (2000) 634.